Systematic Review Article: Total ankle arthroplasty and ankle arthroplasty affect the biomechanics and pain of the midfoot differently: a systematic review

Khosro Kolahdouzan [1], Behrooz Nazari[2]®

[1]Instructor of Anesthesiology, Department of Anesthesiology and Operating Room, School of Allied Medical Sciences, Tabriz University of Medical Sciences, Tabriz, Iran. (ORCID: 0000-0003-4787-7814)
[2]Assistant Professor of Orthopedics, Department of Orthopedics, School of Medicine, Tabriz University of Medical Sciences, Tabriz, Iran.(Corresponding author: ORCID: 0000-0002-7418-7045)

ABSTRACT

Ankle arthroplasty and total ankle arthroplasty are two important treatments for end-stage degenerative ball. Its results on the biomechanics of the medial foot are not sufficient to determine which is better. This study compared the biomechanical parameters of feet treated with ankle arthrodesis, feet treated with total ankle arthroplasty, and healthy feet using statistical analysis. A validated tripod finite element model was designed to simulate the stance phase of gait. The results showed that total ankle arthroplasty provides more stable plantar pressure distribution than ankle arthrodesis. Among all replacements, the mean scaphoid joint had the highest contact pressure of 3.17 MPa. Surgery does not result in deep subscalar fusion. In both surgical models, an increase was achieved in the maximum metatarsals, especially in the second and third metatarsals. This study allows us to look at the internal biomechanics of foot defects and feet treated with total ankle arthroplasty and ankle arthrodesis during walking.

Corresponding Author: Behrooz Nazari (Nazari-berooz@gmail.com)

Introduction

Ankle arthrodesis and total ankle arthroplasty (TAA) are two important methods in the treatment of end-stage degenerative ankle arthritis. Although effective for most patients, both methods can cause many problems. Considered the gold standard of treatment, Ankle Arthrodesis removes joints that can cause fractures, slips, nonunions, degeneration of adjacent joints, and foot pain [1-3]. TAA is recommended as an alternative because it protects the joints, but problems such as fractures, implants, and intercourse often occur. The study on gait analyses, cadaveric experiments physical examination, radiological examination, and pain/function scores compared the functional outcomes and complications of the two surgical treatments [4].

Computational models of the human foot and ankle were used to explore the biomechanics of surgery. A three-dimensional finite element (FE) model of the ankle joint was developed to compare the stability and stress of different models in bone and joint [5-7]. FE models of bone were created to evaluate the biomechanical position of the bone and intramedullary screws and to analyze the pressure on the bone and nail during ankle surgery [8]. A specific TAA model has been developed to understand systolic pressure and implant kinematics, the relationship between prosthetic materials, failure of polyethylene materials, bone healing process after TAA, implant pressure and bone-bone stress. These studies provided information on the biomechanical effects of TAA and ankle sprains, but were performed separately, making it difficult to directly compare the two procedures.

Since the model is also created to directly represent the operation area, it is not possible to evaluate the unilateral effect of these operations on the entire foot [9-11]. Models with a better understanding of foot anatomy will be able to simulate more complex behaviors. The aim of this study was to compare the biomechanical effects of TAA and ankle sprains on the foot using a unique design that represents most of the foot and ankle parts of the body [12].

Negative foot, TAA foot, and ankle fusion foot were used to simulate the stance phase of walking and the biomechanical parameters were compared with our model [13-15]. It has been found that the spread of fat in the feet causes all joints to change, and the joints that cause changes during walking cause stress pressure on the bones, chest distribution and deformation of the feet [16].

Material and Methods

A FE model of the entire foot joint was created by reconstructing 0.625 mm resolution and 2 mm aperture MR images of the right side of the foot of a 164 cm tall, 54 kg woman. Subjects had no history of lower extremity musculoskeletal injury or pathology [17-19]. The geometry of 28 bones and several encapsulated tissues was reproduced in MIMICS (Materialise, Leuven, Belgium). As shown in Figure 1, bone and tissue together form a complete heel. ABAQUS in a finite element package (Dassault Systèms Simulia Corp., [20] Providence, RI, USA). The plantar fascia and ligaments are simulated using only tension lines connecting the bony attachment points. There are nine extrinsic muscle groups: Achilles tendon and triceps calf, tibialis anterior, tibialis posterior, peroneus longus, peroneus brevis, flexor hallucis longus, flexor digitorum longus, extensor hallucis longus and extensor digitorum longus. Each muscle group is formed by connecting the endpoints of the bones using axial connectors that allow the use of the muscles [21-23]. The joints of the bones are fixed to the friction surface, and asymmetric contact is used to represent the cartilage of the joints. Two layers of slabs are built and bonded together in one of the foundations, the top layer represents the ground stone and the bottom layer is placed on a rigid body to allow better blocking of the reaction in the ground [24-26]. The soil consists of concrete with Young's modulus (E) and Poisson's ratio (v) of 17000MPa and 0.1, respectively. bone (E 7300 MPa, v 0.3), ligament (E 260 MPa, cross-sectional area 0.3 mm2) and plantar fascia (E 350 MPa, cross-sectional area 58.6 mm2) are considered homogeneous, isotropic and linear elastic materials [27], while most soft tissue structures

are non- linear and hyperelastic. The hyperelastic behavior is represented by a quadratic polynomial strain energy expression.

The perfect model of TAA Fused Ankle Foot is obtained by replacing the joints of the entire foot model [28-30]. A three-stage total ankle arthroplasty (STAR, Scandinavian Total Ankle Arthroplasty) (Figure 1) was implanted in the model to simulate the TAA foot. According to the surgical procedure, the prosthesis has a tibial plate, a talar component, and a movable bed, each in its place, to change the ankle model. Moving bearings are placed between the tibial and talar components to allow them to slide while connecting to the cross section of the tibia and talus, respectively [31-33]. The contact material is configured so that there is no "surface to surface" friction [34].
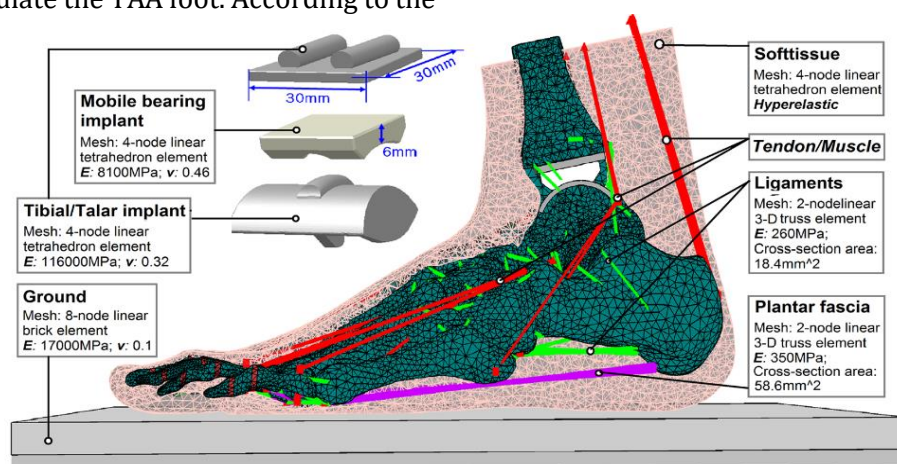

Figure 1. Finite element model of the foot and ankle with total ankle arthroplasty, and parameters of material properties and mesh

The dimensions of the tibial plate and talus components are small (30〉mm〉 × 30 mm) and very small (28 mm〉 × (29mm), respectively. The thickness of the movable bearing is 6 mm. Young's modulus and Poisson's ratio of cobalt-chromium-molybdenum alloy tibial plate and talar prosthesis were set as 116000 MPa and 0.32, respectively. live load is set to 810MPa and 0.46 represents the properties of UHMWPE. All three elements are subdivided into 4-node linear tetrahedral elements [35].

Ankle Arthrodesis is a surgery that removes the cartilage from the joint and turns the talus and tibia into a single bone without affecting other bones or soft tissues. This surgery can be performed with various surgical techniques (open or arthroscopic) and reconstructive techniques (internal or external), all with the aim of limiting the same joint. To represent the mechanism, the interaction of the heel in the FE model was changed from a frictionless "surface-to-surface" connection to a "spin" connection; in ankle arthrodesis, all other bone and soft tissues, including mesh and medical equipment is the same as the whole foot model [36-38].

Obtain the parameters and loading of the experimental game by analyzing the gait of the same subject using a full-footed phantom. Gait analysis was performed in a 10 m walking biomechanics laboratory equipped with eight cameras (Vicon, Oxford Metrics, Oxford, UK) and two platforms (AMTI, Advanced Mechanical Technology, Inc., Watertown, Massachusetts, USA) [39]. To collect kinetic and kinematic data, 16 reflex marks were placed on the subject's buttocks, identifying seven segments: stomach, two thighs, two stomachs, and two feet. High resolution scanning (F-Scan, TekScan Inc, Boston, MA, USA) was used to measure the scattering of plants during model validation. Each sensor is trimmed to fit the size of the foot and two tapes are used to connect the two sensors together on the foot [40].

Subjects were asked to walk at their own pace, with a different speed for each foot. It took ten attempts to walk. During this procedure, the

trajectory, ground reaction force, and plantar pressure of each foot are recorded. Calculate the angle of the abdomen to the floor by plotting the trajectory of the calf. Data from these 10 trials were resampled and sample sizes were based on the average ground response and calf-to-ground angle of the 10 trials. Figure 2 shows the average ground response force curve for 10 brisk walking trials and three accelerations. The vertical curve of the support line shows two peaks and a valley, the first peak appears at 17.5% of the support level, 48% of the valley and the second peak appears at 76% of the level

support. Joint research now speaks of ground response and curve in our time. Three simulated periods, the first peak period, the middle period, and the second period. Muscle Fi was estimated from muscle tissue section (PCSA) and electromyography (EMG) data from transport, that is, EMG lines of force close to 25 N/cm2⟩ muscles increase gi. EMG data from studies were normalized to remove the effect of individual differences. Use ground angle, ground reaction, and triple muscle gain as constraints and loads for the model [41].
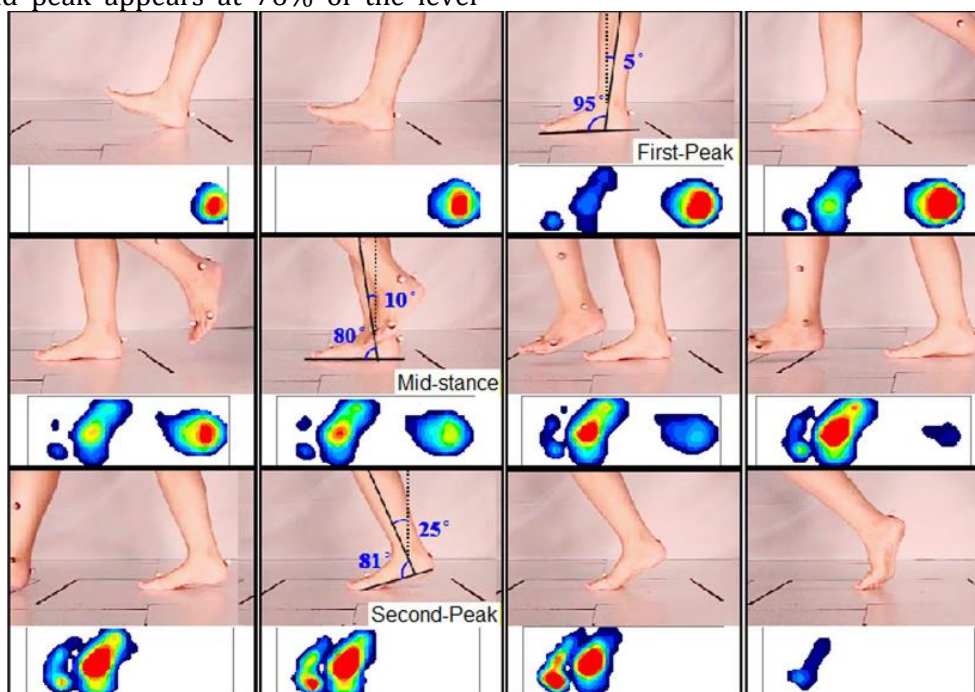

Figure 2 Foot positions, plantar pressure distribution, and curves of ground reaction forces during the stance phase

Bad foundation models are validated by comparing finite element estimates and experimental measurements. One comparison is the liver implant between the estimated FE in the walking test and the F-Scan measurement, and the other comparison is the comparison between the estimated FE in the cadaver test.

Results

Assess the biomechanical properties of the foot and ankle during walking using a properly designed phantom. Biomechanical parameters such as bad foot, plantar pressure between TAA foot and ankle, deep joint, deep strength,

metatarsal stress, wing and step change were compared. in the province. Plantar pressure distributions were compared between FE estimates and F-scan measurements for the three conditions, including equilibrium, first peak, and second peak time. In balance, the mean stresses in the forefoot and hindfoot for FE estimation are 0.051>MPa and 0.168>MPa and 0.058>MPa and 0, respectively. 157 MPa in experimental tests. At the rear leg of the first top element these values are 0.3 MPa and 0.307 MPa in FE estimation and experimental measurement, respectively [42]. At the second peak, the mean plantar pressure in the forefoot

is 0. FE estimates and experimental values are 227 MPa and 0.223 MPa, respectively. To compare the scaphoid articulation in the FE model with that measured in the cadaver experiment, the FE model and the cadaver foot were subjected to the same area and load. The mean pressure was estimated to be 0.25 MPa by the finite element method and 0 by physical measurement [43].

The triple plantar pressure blade of the tripod model is shown in Figure 3. In the negative sample the maximum pressure is 0.332MPa, 0.683MPa and 0 respectively. For the TAA foot sample, the pressure of the first peak of the middle and second peaks is 683 MPa and 0, respectively. 930MPa is 9%, 14% and 36% higher than all samples. It should be noted that there is a greater difference in maximum plantar pressure in the ankle fusion foot than in the TAA foot. The height of the TAA foot is not different from the bad foot, and the heel fusion is three degrees ahead, similar to the bad foot, by 15mm, 16mm and 5mm.
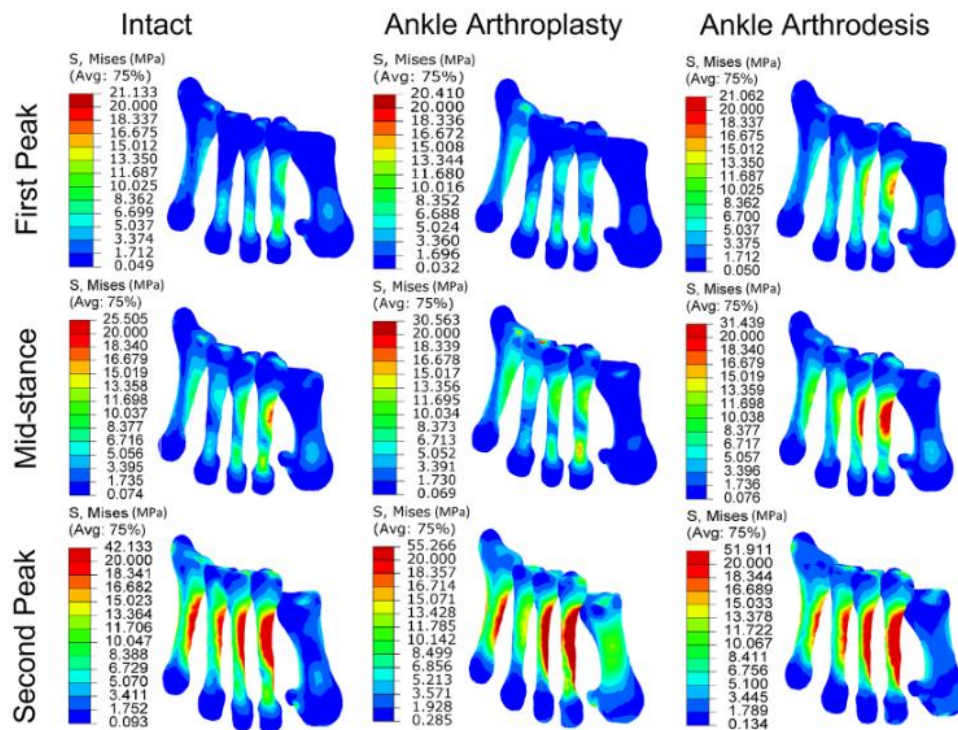

Figure 3. CPPD and the location of COP among the IFMTAA model, and AAT model

During the first peak flow, the contact between the subtalar joint (1), the calcaneocuboid joint (3), and the fourth tarsal metatarsal joint (10) is reduced relative to the working biped model. Compared with the TAA and normal foot model, there was a decrease in contact points of 10 of 11 normal joints, and a 21.7% increase in only the 5th tarsal metatarsal joint. Compared with the ankle joint of the whole foot model, there was good contact in 8 of the 11 joints, including the first talonavvicular joint (2), medial navicular (4), medial navicular (5), lateral navicular bone. (6). Tarsus metatarsal (7), second tarsus metatarsal (8), third tarsus metatarsal (9), fifth tarsus metatars (11), 50. 5%, 31. 1%, 41.6%, 80.3%, 21.9%, 49.7%, 62%. 8% and 13.8%, respectively. At the onset of the peak, the maximum contact of all structures takes place on the pair of talonavvicula, which is 1.

The contact of the working feet between the subtalar (1), the calcaneocuboid (3) and the fifth tarsal metatarsal joint (11) decreases in the mid-term compared to the standard foot. Compared with the TAA and normal foot model, 8 out of 11 joints decreased first contact except the

navicular side (6), the third tarsal metatarsal increased 44.3%, and early contact decreased 15.1% and 6.3% (9) (9) fourth metatarsals (10). Compared with joint arthrodesis and full foot models, talar navicular (2), medial navicular (4), medial navicular (5), lateral navicular (6), 1st tarsal metatarsal (7), second tarsal metatarsal (8), and third tarsal metatarsal (9) increased 39.6%, 23.9%, 41.8%, 64%. 7% and 24%, respectively. 4%, 30.9% and 51.4%, respectively. In mid stance, the greatest contact of all structures occurs on the No. 1 talar navicular muscle. 59 MPa in the fused ankle model.

During the second peak flow, the contact between the subtalar joint (1) of the working feet and the fifth tarsal metatarsal joint (11) decreases compared to the standard foot. The subtalar joint (1), the navicular joint (5), and the fifth tarsal metatarsal joint (11) had less contact than the TAA whole foot model. Tarsal navicular (2), ankle navicular (3), medial cuneiform (4), lateral cuneiform (6), first tarsal metatarsal (7), second tarsal metatarsal (8), third tarsal metatarsal (9), fourth tarsal metatarsal bones (10), 20.5%, 4.1%, 67.4%, 3.6%, 44.0%, 15.6%, 14.7% and 37%. Compared with arthrodesis of the 5% Whole foot model, the former showed the talar navicular bone (2), medial muscle (4), medial muscle (5), medial muscle (6), navicular bone 1 tarsal metatarsal (7), respectively.), 2nd tarsal metatarsal bone (8), 3rd tarsal metatarsal bone (9), 4th tarsal metatarsal bone (10), 6.8%, 3.9%, 7.3%, 11. 6%, 11.6%, 9.7%, 2.0% and 63%, respectively. 1% respectively. In the second period of the current period, the maximum contact of each sample occurs at the joint (4) of the TAA sample foot, which is 3.17 > MPa.

In our time, a comparison of the distribution of body weight was made in our example. Force is transmitted from the back to the midfoot via the ankle and ankle. Power is 0.34.0. Body weight was changed 33-fold and 0.58-fold by the tanarroroid joint in the abnormal foot model, TAA model, and ankle model. Also, strengths are 0.09, 0.08 and 0.In our model, 06 times the body weight is spread on the wrist. Power is transferred from the midfoot to the forefoot via the five tarsal metatarsal joints. Middle to outward, the first to third metatarsals are the

midway, and the fourth to fifth metatarsals are the way. The average value is 0.23, 0.19 and 0, respectively. Our standard is 34 times body weight, then changed to 0.11, 0.11 and 0.07 times body weight.

The weight of the tanarovoid joint from the hindfoot to the midfoot was 0.48, 0.53 and 0.76 body weight, respectively, and the weight of the calcaneocuboid joint was 0.12.0. In our example, this is 11 and 0.10 times the weight, respectively. The mean fat distribution in the midfoot and forefoot joints is 0.34.0.32i0, do it. Three samples were 46 times body weight, 0.19, 0.17, 0.16 times body weight. In our model, between the ankle and midfoot, the tanarovoid joints carry 0.95, 1.15, and 1.07 times the body weight, respectively, and the calcaneocuboid joints carry 0.15.0 times the body weight. 15 and 0.14 times the body weight load, respectively. The distribution between the middle and lower joints is 0.69, 0.77 and 0, respectively. At the first peak, the maximum stress was 21.1 MPa, 20.4 MPa, and 21.1 MPa for the foot model, TAA model, and ankle fusion model, respectively. The TAA model has up to 3 more legs than the standard model. 32% reduction with little change in joints. The average maximum pressure of the tripod sample is 25.5 MPa, 30.6 MPa and 31.4 MPa, respectively. Compared to the whole foot model, the maximum is 20% higher for the TAA model and 23.1% higher for the ankle model. The maximum in the second period is 42.1 > MPa, 55.3 > MPa and 51 respectively. Compared with the change of the angle of the TAA foot, the ankle fusion foot, and the negative forefoot between the first peak and the mid-period, the change of the second peak is different in three ways. The feet of all three models are in the same position with a 30° deviation from the vertical. The angle between ground and axis along the first ray (medial cuneiform, first metatarsal, and first phalanx) is 28° in the foot model, 35° in the TAA model, and 44° in the ankle fusion model.

Discussion

The ankle complex, a multifunctional biomechanical structure, provides support, thrust and alignment to the body. Surgery

changes the components of the complex, which causes deviations in the kinematics and dynamics of the medial foot and plantar loads. In this study, the biomechanical results of the whole joint and joint were examined and compared in terms of joint stiffness, body pressure, bone tension and orientation.

Plantar pressure is an important measure of clinical outcome and is used to improve understanding of foot function and the effectiveness of medical and surgical treatment for the foot. Estimates based on the results of this study support previous findings that TAA does not increase or change height, while the heel rises and pushes height forward. In the middle of the first peak, the TAA foot makes the heel the same as the bad foot, while the entire heel and ankle fusion foot should be replaced starting from the forefoot, adding to the ankle dorsiflexion and tibial orientation during walking. front. As seen in this study, this equation positions the heel at half the height of the other foot. herefore, the pressure peak in the ankle fusion foot occurs at the first metatarsal head of the forefoot rather than the heel region as in the well and TAA foot. Increased plantar pressure can cause discomfort during strenuous activity and increase the risk of back pain. Most patients adapt to the changes and minimize adverse effects through physical therapy, walking speed, and cadence.

While the correlation coefficient of the TAA foot is close to the negative foot in the first peak and mid-period, it changes rapidly in the second peak. Ankle arthrodesis causes greater impact in the first half of the stance phase, while providing stable biomechanics in the second half. In the first peak and middle period, the connection between the ankle joint and the scaphoid joint is weak and TAA is higher than the foot. A higher prevalence indicates a higher risk of changes in the joint after resection. The arthropathy observed after the ankle as well as the talar navicular, cuneiform and tarsal metatarsals in this study was consistent with the prediction of this study. The fact that neither TAA nor ankle sprains are associated with an increase in subtalar arthropathy supports the hypothesis that subtalar arthropathy is the most common cause of degeneration after ankle arthrodesis.

The range of motion of the ankle is smaller in TAA and ankle sprains than in the foot, and it is minimal in arthrodesis in ankle sprains. This is because a three-layer ankle prosthesis protects part of the ankle, while total ankle arthrodesis restricts the ankle. This finding is consistent with kinematic studies of TAA and ankle immobilized feet. In both foot surgery models, the forefoot range of motion is greater than the bad foot, and the most common side effects are seen in the ankle. As predicted in this study, during joint arthrodesis, the ankle first bends the tibia, causing further deformation of the forefoot. This will represent payment for cooperation. The current configuration of our joints theoretically allows some degree of dorsiflexion and plantarflexion in the sagittal plane, but completely limits valgus/varus movement in the frontal plane. But the tilted axis of the ankle indicates movement in three planes. Gait development depends on the coordination of the joints in the body, especially the feet and ankles. Each room is tailored to the job situation to protect feet and ankles at work. Limited range of motion in the sagittal plane may be the result of valgus/varus restriction. The results expected to predict how foot biomechanics, particularly the inside of the foot, are differently affected by total ankle and ankle fusion surgery, are beyond the limitations of the method. your foot. .in a real Down state. to work. First, the computational model is based on simplicity and logic. In the FE model, the bone, cortical and trabecular components are reconstructed without separation and are characterized by homogeneous, isotropic and linear elastic properties. Second, the limitations and load applied to the ankle sprain and TAA foot are similar to the non-sensitive foot. For comparison, patients should return to normal after surgery, although some patients may adjust to their comfort. Further research should include ankle motion analysis and TAA patients to improve outcomes. Third, the force and spread from direct bone contact, which can be improved using new visible material from the subperiosteal region.

When character is represented using bone to bone, the shape of the cartilage can be improved using cartilage. In order to examine the true

biomechanics of the inner foot in future studies, the computational model will be modified to include changes in subperiosteal and cartilage structures and bone structure. Improvements in the finite element model will continue in the field. The method and validity of the model were increased by using the contact area and deformation in the cartilage. In addition, this model was created by a woman in an effort to represent the working behavior of the foot, so individual differences were not taken into account. For example, differences in foot weight, weight, or gait lead to changes in some outcomes of foot biomechanics. In further research, simulations will be performed to simulate continuous data in triplicate, and the data will be validated by comparison with non-three time steps.

Conclusion

Neither TAA nor ankle arthrodesis fully protect the trunk of the ankle, thus causing a deflection of the ankle, which is compensated by a change in the forefoot. The work of this segment is related to communication and bone connection. Comparing these parameters with normal foot models and TAA ankle arthrodesis results in better definition of hip and ankle joints in the sagittal plane than ankle arthrodesis. The greatest and greatest contact pressure difference occurs at the medial navicular joint of the TAA foot. The procedure does not add stress to the subtalar joint.

References

[1]   Yazdanian M, Rahmani A, Tahmasebi E, Tebyanian H, Yazdanian A, Mosaddad SA. Current and Advanced Nanomaterials in Dentistry as Regeneration Agents: An Update. Mini Reviews in Medicinal Chemistry. 2021;21(7):899-918. [Crossref], [Google Scholar], [Publisher]

[2]   Tosan F, Rahnama N, Sakhaei D, Fathi AH, Yari A. Effects of doping metal nanoparticles in hydroxyapatite in Improving the physical and chemical properties of dental implants. Nanomedicine Research Journal. 2021 Nov 1;6(4):327-36.[Crossref], [Google Scholar], [Publisher]

[3]   Tahmasebi E, Alam M, Yazdanian M, Tebyanian H, Yazdanian A, Seifalian A, et al. Current biocompatible materials in oral regeneration: a comprehensive overview of composite materials. Journal of Materials Research and Technology. 2020;9(5):11731-55. [Crossref], [Google Scholar], [Publisher]

[4]SE Ahmadi, M Farzanehpour, AMM Fard, MM Fard, HEG Ghaleh, Succinct review on biological and clinical aspects of Coronavirus disease 2019 (COVID-19), Romanian Journal of Military Medicine, 2022,356-365, [Google Scholar], [Publisher]

[5]   Saliminasab M, Jabbari H, Farahmand H, Asadi M, Soleimani M, Fathi A. Study of antibacterial performance of synthesized silver nanoparticles on Streptococcus mutans bacteria. Nanomedicine Research Journal. 2022 Oct 1;7(4):391-6.[Google Scholar], [Publisher]

[6]SA Mahkooyeh, S Eskandari, E Delavar, M Milanifard, FE Mehni, Chemical laboratory findings in children with covid-19: A systematic review and meta-analysis, Eurasian Chemical Communications, 2022, 338-346, [Crossref], [Google Scholar], [Publisher]

References

[7]Nazari B, Amani L, Ghaderi L, Gol MK. Effects of probiotics on prevalence of ventilator-associated pneumonia in multitrauma patients hospitalized in neurosurgical intensive care unit: a randomized clinical trial. Trauma Monthly.2020; 25(6): 262-268. [Crossref], [Google Scholar], [Publisher]

[8]   Namanloo RA, Ommani M, Abbasi K, Alam M, Badkoobeh A, Rahbar M, et al. Biomaterials in Guided Bone and Tissue Regenerations: An Update. Advances in Materials Science and Engineering. 2022;2022:2489399. [Crossref], [Google Scholar], [Publisher]

[9]Mosharraf R, Molaei P, Fathi A, Isler S. Investigating the Effect of Nonrigid Connectors on the Success of Tooth-and-Implant-Supported Fixed Partial Prostheses in Maxillary Anterior Region: A Finite Element Analysis (FEA). International Journal of Dentistry. 2021 Nov 12;2021: 5977994.[Crossref], [Google Scholar], [Publisher]

[10] Mosaddad, SA, Abdollahi Namanloo, R, Ghodsi, R, Salimi, Y, Taghva, M, Naeimi Darestani, M. Oral rehabilitation with dental implants in patients with systemic sclerosis: a systematic review. Immun Inflamm Dis. 2023; 11:e812. [Crossref], [Google Scholar], [Publisher]

[11] Mosaddad SA, Yazdanian M, Tebyanian H, Tahmasebi E, Yazdanian A, Seifalian A, et al. Fabrication and properties of developed collagen/strontium-doped Bioglass scaffolds for bone tissue engineering. Journal of Materials Research and Technology. 2020;9(6):14799-817. [Crossref], [Google Scholar], [Publisher]

[12] Mosaddad SA, Salari Y, Amookhteh S, Soufdoost RS, Seifalian A, Bonakdar S, et al. Response to Mechanical Cues by Interplay of YAP/TAZ Transcription Factors and Key Mechanical Checkpoints of the Cell: A Comprehensive Review. Cell Physiol Biochem. 2021;55(1):33-60.[Crossref], [Google Scholar], [Publisher]

[13] Mosaddad SA, Rasoolzade B, Namanloo RA, Azarpira N, Dortaj H. Stem cells and common biomaterials in dentistry: a review study. Journal of Materials Science: Materials in Medicine. 2022;33(7):55. [Crossref], [Google Scholar], [Publisher]

[14] Mosaddad SA, Namanloo RA, Aghili SS, Maskani P, Alam M, Abbasi K, et al. Photodynamic therapy in oral cancer: a review of clinical studies. Medical Oncology. 2023;40(3):91. [Crossref], [Google Scholar], [Publisher]

[15] Mosaddad SA, Gheisari R, Erfani M. Oral and maxillofacial trauma in motorcyclists in an Iranian subpopulation. Dental Traumatology. 2018;34(5):347-52. [Crossref], [Google Scholar], [Publisher]

[16] Mosaddad SA, Beigi K, Doroodizadeh T, Haghnegahdar M, Golfeshan F, Ranjbar R, et al. Therapeutic applications of herbal/synthetic/bio-drug in oral cancer: An update. Eur J Pharmacol. 2021;890:173657.[Crossref], [Google Scholar], [Publisher]

[17] Moharrami M, Nazari B, Anvari HM. Do the symptoms of carpal tunnel syndrome improve following the use of Kinesio tape? Trauma Monthly.2021; 26(4):228-234. [Crossref], [Google Scholar], [Publisher]

[18] Moharrami M, Anvari HM, Gheshlaghi LA, Nazari B. Preoperative education for pain relief after the lower limb joint replacement surgery: A systematic review and meta-analysis. Trauma Monthly; 26(1):52-60. [Crossref], [Google Scholar], [Publisher]

[19] Mobaraki-Asl N, Ghavami Z, Gol MK. Development and validation of a cultural competence questionnaire for health promotion of Iranian midwives. Journal of education and health promotion. 2019;8:179. [Crossref], [Google Scholar], [Publisher]

[20] Maalekipour M, Safari M, Barekatain M, Fathi A. Effect of adhesive resin as a modeling liquid on elution of resin composite restorations. International Journal of Dentistry. 2021 Dec 28;2021. 3178536.[Crossref], [Google Scholar], [Publisher]

[21] Haghdoost M, Mousavi S, Gol MK, Montazer M. Frequency of Chlamydia trachomatis Infection in Spontaneous Abortion of Infertile Women During First Pregnancy Referred to Tabriz University of Medical Sciences by Nested PCR Method in 2015. International Journal of Women's Health and Reproduction Sciences. 2019; 7(4): 526-30. [Google Scholar], [Publisher]

[22] H Danesh, A Bahmani, F Moradi, B Shirazipour, M Milanifard, Pharmacological Evaluation of Covid 19 Vaccine in Acute and Chronic Inflammatory Neuropathies,

Journal of Medicinal and Chemical Sciences, 2022, 561-570, [Crossref], [Google Scholar], [Publisher]

[23] Golfeshan F, Mosaddad SA, Ghaderi F. The Effect of Toothpastes Containing Natural Ingredients Such As Theobromine and Caffeine on Enamel Microhardness: An In Vitro Study. Evidence-Based Complementary and Alternative Medicine. 2021;2021:3304543. [Crossref], [Google Scholar], [Publisher]

[24] Golfeshan F, Mosaddad SA, Babavalian H, Tebyanian H, Mehrjuyan E, Shakeri F. A Summary of Planarian Signaling Pathway for Regenerative Medicine. Proceedings of the National Academy of Sciences, India Section B: Biological Sciences. 2022;92(1):5-10. [Google Scholar], [Publisher]

[25] Golfeshan F, Ajami S, Khalvandi Y, Mosaddad SA, Nematollahi H. The Analysis of the Differences between the Influence of Herbal Mouthwashes and the Chlorhexidine Mouthwash on the Physical Characteristics of Orthodontic Acrylic Resin. Journal of Biological Research - Bollettino della Società Italiana di Biologia Sperimentale. 2020;93(1). [Google Scholar], [Publisher]

[26] Gheisari R, Resalati F, Mahmoudi S, Golkari A, Mosaddad SA. Do Different Modes of Delivering Postoperative Instructions to Patients Help Reduce the Side Effects of Tooth Extraction? A Randomized Clinical Trial. Journal of Oral and Maxillofacial Surgery. 2018;76(8):1652.e1-.e7.[Crossref], [Google Scholar], [Publisher]

[27] Gheisari R, Doroodizadeh T, Estakhri F, Tadbir A, Soufdoost R, Mosaddad S. Association between blood groups and odontogenic lesions: a preliminary report. Journal of Stomatology. 2019;72(6):269-73. [Crossref], [Google Scholar], [Publisher]

[28] Fathi A, Giti R, Farzin M. How different influential factors affect the color and translucency of y-ztp: a review of the literature. Annals of Dental Specialty. 2018 Jul 1;6(3):338-41.[Google Scholar], [Publisher]

[29] F Elmi Sadr, Z Abadi, N Elmi Sadr, M Milani Fard, The Risk for SARS-Cov-2 Virus Contamination through Surgical Smoking and Aerosolization by Laparoscopic Surgery: A Systematic Review, Annals of the Romanian Society for Cell Biology 25 (1), 6839 – 6852, [Google Scholar], [Publisher]

[30] Eydi M, Golzari SEJ, Aghamohammadi D, Kolahdouzan K, Safari S, Ostadi Z. Postoperative management of shivering: A comparison of pethidine vs. ketamine. Anesthesiology and Pain Medicine;2014: 4(2),e15499 [Crossref], [Google Scholar], [Publisher]

[31] Eidy M, Ansari M, Hosseinzadeh H, Kolahdouzan K. Incidence of back pain following spinal anesthesia and its relationship to various factors in 176 patients. Pakistan Journal of Medical Sciences.2010; 26(4):778-781. [Google Scholar], [Publisher]

[32] Eidi M, Kolahdouzan K, Hosseinzadeh H, Tabaqi R. A comparison of preoperative ondansetron and dexamethasone in the prevention of post-tympanoplasty nausea and vomiting. Iranian Journal of Medical Sciences.2012; 37(3):166-172. [Google Scholar], [Publisher]

[33] Eghdam-Zamiri R, Gol MK. Effects of ginger capsule on treatment of nausea and vomiting in patients receiving cisplatin undergoing mastectomy: a randomized clinical trial. The Iranian Journal of Obstetrics, Gynecology and Infertility. 2020;22(11): 15-21. [Crossref], [Google Scholar], [Publisher]

[34] Ebadian B, Fathi A, Khodadad S. Comparison of the effect of four different abutment screw torques on screw loosening in single implant-supported prosthesis after the application of mechanical loading. International Journal of Dentistry. 2021 Jul 19;2021: 3595064.[Google Scholar], [Publisher]

[35] Dargahi R, Nazari B, Dorosti A, Charsouei S. Does coronavirus disease affect sleep disorders in the third trimester of

pregnancy in women with low back pain? International Journal of Women's Health and Reproduction Sciences.2021; 9(4):268-273. [Google Scholar], [Publisher]

[36] Darestani MN, Houshmand B, Mosaddad SA, Talebi M. Assessing the Surface Modifications of Contaminated Sandblasted and Acid-Etched Implants Through Diode Lasers of Different Wavelengths: An In-Vitro Study. Photobiomodulation, Photomedicine, and Laser Surgery. 2023. [Crossref], [Google Scholar], [Publisher]

[37] Ansari lari H, Jahed SH, Abbasi K, Alam M, Alihemmati M, Ghomi AJ, et al. In Vitro Comparison of the Effect of Three Types of Heat-Curing Acrylic Resins on the Amount of Formaldehyde and Monomer Release as well as Biocompatibility. Advances in Materials Science and Engineering. 2022;2022:8621666. [Google Scholar], [Publisher]

[38] Aghili SS, Pourzal A, Mosaddad SA, Amookhteh S. COVID-19 Risk Management in Dental Offices: A Review Article. Open Access Maced J Med Sci. 2022 Nov 04; 10(F):763-772. [Crossref], [Google Scholar], [Publisher]

[39] Afshari A, Shahmohammadi R, Mosaddad SA, Pesteei O, Hajmohammadi E, Rahbar M, et al. Free-Hand versus Surgical Guide Implant Placement. Advances in Materials Science and Engineering.

2022;2022:6491134. [Crossref], [Google Scholar], [Publisher]

[40] Afshari A, Mosaddad SA, Alam M, Abbasi K, Darestani MN. Biomaterials and Biological Parameters for Fixed-Prosthetic Implant-Supported Restorations: A Review Study. Advances in Materials Science and Engineering. 2022;2022:2638166. [Crossref], [Google Scholar], [Publisher]

[41] Abdollahi MH, Foruzan-Nia K, Behjati M, Bagheri B, Khanbabayi-Gol M, Dareshiri S and et al. The effect of preoperative intravenous paracetamol administration on postoperative fever in pediatrics cardiac surgery. Nigerian medical journal: journal of the Nigeria Medical Association.2014; 55(5): 379. [Crossref], [Google Scholar], [Publisher]

[42] A Susanabadi, et al., Evaluating the Outcome of Total Intravenous Anesthesia and Single Drug Pharmacological to Prevent Postoperative Vomiting: Systematic Review and Meta-Analysis, Annals of the Romanian Society for Cell Biology, 2021, 25 (6), 2703-2716, [Google Scholar], [Publisher]

[43] A Susanabadi, et al., A Systematic Short Review in Evaluate the Complications and Outcomes of Acute Severe of Pediatric Anesthesia, Journal of Chemical Reviews, 2021, 3 (3), 219-231, [Crossref], [Google Scholar], [Publisher]